Spectral, spatial, and temporal characteristics of underwater ambient noise in the Beaufort Sea in 1994 and 2016

Citation: R. Chen, A. Poulsen, H. Schmidt; Spectral, spatial, and temporal characteristics of underwater ambient noise in the Beaufort Sea in 1994 and 2016. J. Acoust. Soc. Am. 1 February 2019; 145 (2): 605–614.

As Published: 10.1121/1.5088601

Publisher: Acoustical Society of America

Persistent URL: https://hdl.handle.net/1721.1/154272

Version: Final published version: final published article, as it appeared in a journal, conference proceedings, or other formally published context

FEBRUARY 01 2019

Spectral, spatial, and temporal characteristics of underwater ambient noise in the Beaufort Sea in 1994 and 2016

R. Chen; A. Poulsen; H. Schmidt

J. Acoust. Soc. Am. 145, 605–614 (2019)
https://doi.org/10.1121/1.5088601

Spectral, spatial, and temporal characteristics of underwater ambient noise in the Beaufort Sea in 1994 and 2016

R. Chen,[1,a)] A. Poulsen,[2] and H. Schmidt[1]
[1]*Mechanical Engineering, Massachusetts Institute of Technology, Cambridge, Massachusetts 02139, USA*
[2]*Modeling, Simulation and Signal Processing Department, Applied Physical Sciences, Lexington, Massachusetts 02478, USA*

(Received 26 October 2018; revised 11 January 2019; accepted 11 January 2019; published online 1 February 2019)

Climate induced changes in the Arctic Ocean have severely impacted underwater acoustic communication and navigation; understanding underwater noise characteristics is critical to improving the performance of these operations. Ambient noise from the Beaufort Sea recorded in experiments more than 20 years apart (SIMI94 and ICEX16) are compared to determine differences that may be attributed to the region's rapidly changing environment. Spectral comparison shows noise within 20–350 Hz is ∼30 dB louder in 1994 than 2016; however, this is likely due to higher array self noise during SIMI94. Beamforming results show ambient noise vertical directionality is focused near the horizontal during SIMI94 but more spread in elevation during ICEX16, with a robust noise notch at the horizontal. Numerical modeling demonstrates that this difference may be attributed to ambient noise during ICEX16 being dominated by surface noise sources at discrete ranges rather than the historical assumption of a continuous and uniform distribution of sources. Temporal statistics of transient ice events show more acoustic activity during SIMI94 than ICEX16 and appear to support the new proposed surface source distribution for ICEX16. © *2019 Acoustical Society of America*.
https://doi.org/10.1121/1.5088601

[JAC] Pages: 605–614

I. INTRODUCTION

Underwater ambient noise in the Beaufort sea region of the Arctic ocean is an intriguing topic of study because of rapid environmental changes in the area. Over the past three decades, the surface ice sheet has thinned[1] and the extent of its coverage has declined.[2] Specifically, the percentage of perennial multi-year ice has decreased; in its place, seasonal first-year ice that is more susceptible to ridging has become more prevalent.[3] Below the ice, an influx of warm water entering the region from the Bering Strait, known as the "Beaufort Lens," sits neutrally buoyant at 60–80 m depth. While this phenomenon has been noted since the 1970s,[4] a recent observation by the Woods Hole Oceanographic Institution (WHOI) Ice-Tethered Profiler program discovered that its intensity has increased and its geographical extent has spread.[5] As a result, the Beaufort Lens disrupts the typical, monotonically increasing Arctic ocean sound speed profile (SSP) by creating a local maximum at its depth (Fig. 1). This change creates a double duct environment, one at the surface and another at approximately 100–200 m depth. The upper duct has a strong upward refracting sound speed profile, significantly increasing sound-ice interactions. The lower duct has been shown to effectively trap sound above 300 Hz.[6,7] The impact of these recent environmental changes on underwater ambient noise still requires further investigation and is the main focus of this paper.

Due to the region's strategic importance, Arctic Ocean underwater ambient noise has been studied extensively. Numerous papers have examined the correlation of ambient noise with environmental stresses such as wind, temperature, ocean current, and air pressure.[8–13] Other research has described spatial and temporal statistical characteristics of the composite ambient noise[14,15] or individual transient events.[16–19] This paper provides a unique perspective on the changes in the ambient noise environment by analyzing and comparing two datasets collected more than 20 years apart at the same location during the same time of the year (Fig. 2). One dataset was recorded in 2016 under current environmental conditions, while the other was recorded in 1994 when more traditional Arctic conditions were still prevalent. The goal of this study is to compare the ambient noise characteristics and identify differences that may be attributed to the changed environment.

The sections of this paper are as follows. Section II describes the two experiments during which the data for this study were collected. Section III compares the spectral characteristics of ambient noise from the two experiments. Section IV explores the spatial differences in their vertical directionality and proposes a model for the surface source distribution during ICEX16. Section V describes the temporal statistics of transient events detected in the datasets. Finally, Sec. VI summarizes the findings and proposes future studies.

II. EXPERIMENTS

A. ICEX16

In March of 2016, The Massachusetts Institute of Technology Laboratory for Autonomous Marine Sensing Systems (MIT-LAMSS), Applied Physical Science Corporation

[a)]Electronic mail: ruic@mit.edu

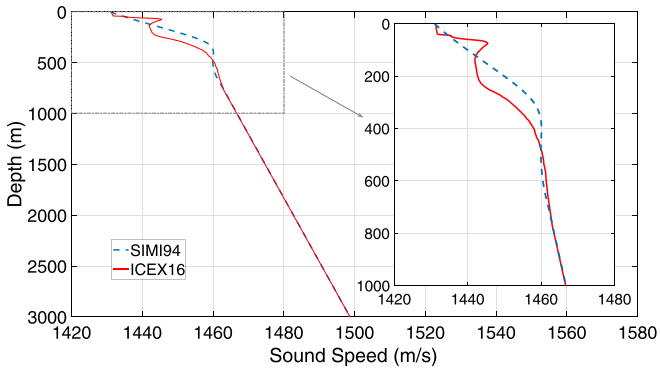

FIG. 1. (Color online) Sound speed profile during SIMI94 (dashed) and ICEX16 (solid).

(APS), Bluefin Robotics, and GobySoft jointly participated in the U.S. Navy's 2016 Ice Exercise (ICEX16) in the Beaufort Sea region of the Arctic ocean. One scientific goal of this collaboration is to characterize climate induced effects on the region's underwater acoustic environment. Continuous ambient noise data were recorded with a 32 element vertical line array (VLA) tethered below a suspended Bluefin 21 autonomous underwater vehicle (AUV) at a sampling rate of 12 000 Hz and 16-bit amplitude quantization under packed ice conditions. The VLA had omni-directional hydrophones with nested spacings of 1.5 and 0.75 m (Fig. 3) and its center was 38 m below the AUV. Two datasets were gathered during the experiment. First, approximately 8 h of ambient noise was recorded with the AUV at the ocean surface (center of the VLA at 38 m depth) in a man-made ice hole on March 13th (Coordinated Universal Time, UTC). About 17 min of each hour of this data were contaminated with loud interferences from a modem used to communicate with the AUV and are thus excluded from analysis, resulting in a net 5.65 h of data at 38 m depth. On March 14th (UTC), more ambient noise data were collected at different water depths by suspending the AUV 25–200 m below the ice hole at ~25 m increments (the center of the array ranged from 63 to 238 m). At each depth, roughly 20 min of data were collected. In this study, results from the array at 138 and 238 m

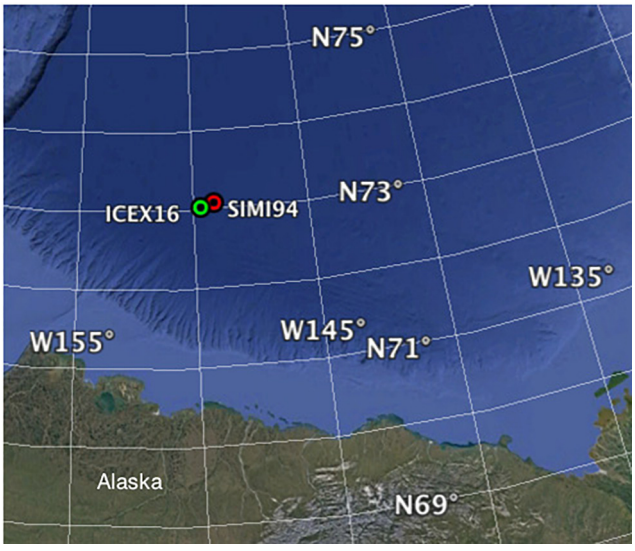

FIG. 2. (Color online) ICEX16 and SIMI94 camp locations.

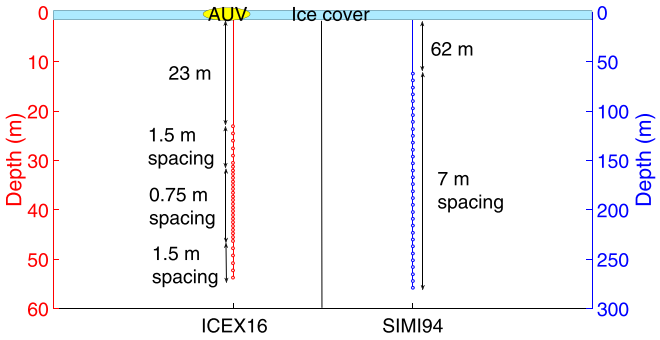

FIG. 3. (Color online) ICEX16 VLA with AUV at the surface and SIMI94 VLA. Note the depth scale difference between left and right.

depth are presented in addition to the longer period of recording at 38 m depth.

B. SIMI94

The Sea Ice Mechanics Initiative (SIMI) was a collective effort between MIT and WHOI to study ice fracturing processes and their environmental correlates during the spring of 1994. Both a cross array and a VLA were deployed at Beaufort Sea under packed ice conditions. Data analyzed in this paper come from the VLA, which had 32 omni-directional channels with 7 m spacing recording continuously at a sampling rate of 1000 Hz (Fig. 3). The top of the array was at 62 m depth. The collected data also had 16-bit amplitude quantization and were bandpass filtered between 1 and 350 Hz (24 dB/octave roll-off at low end, 48 dB/octave roll-off at high end) by the acquisition system and stored on tapes, each roughly 8 h in length. In total, 35 tapes of data were recorded; however, the VLA was only active during tapes 23–32 (from April 18–22 UTC). All tapes had a continuous interference at 60 Hz caused by the camp generators. Many tapes also included strong noise bands at 70 and 80 Hz and greater frequencies. For this study, data from tape 23 were analyzed because this tape contained lower levels of noise interference compared to the rest. Specifically, the first six hours of data are used so that the amount of data analyzed is comparable to data collected during ICEX16 at 38 m depth.

III. SPECTRAL COMPARISON

A. Method

Spectrograms and power spectral density (PSD) estimates are generated to compare the ambient noise spectral characteristics during both experiments [Figs. 4(a), 4(b), and 5]. ICEX16 data collected with the array center at 38 m depth is used for comparison with SIMI94 Tape 23 because of their longer, comparable time scales (as noted, data segments collected at other depths during ICEX16 are only ~20 min long). For a more consistent comparison, data from the lowest hydrophone in the ICEX16 VLA is compared with data from the top hydrophone in the SIMI94 VLA because they are at similar depths: 54 and 62 m, respectively. For ICEX16, the data is segmented into 4096 point Hanning windows with 50% overlap before taking a fast Fourier transform (FFT), which results in a frequency resolution of ~3 Hz. The PSD estimates are sorted by power at each frequency and the median values are plotted.

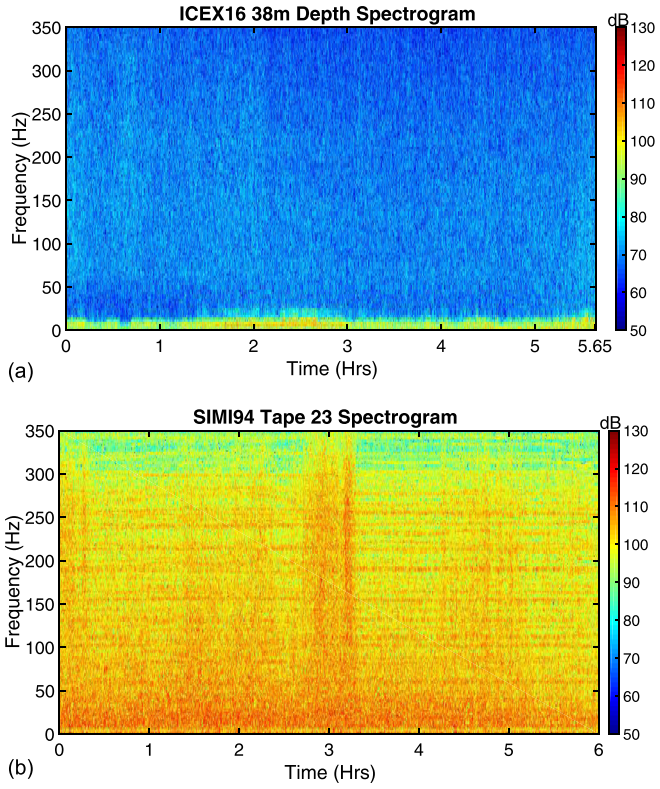

FIG. 4. (Color online) (a) ICEX16 spectrogram. Noise level below 25 Hz is much higher than levels at higher frequencies. (b) SIMI94 spectrogram. Noise level is high at all frequencies; persistent bands are visible at distinct frequencies, which are likely caused by artificial interfering sources due to their narrow bandwidth.

The SIMI94 data are analyzed with the same method; a window length of 512 is used for the FFT to produce a frequency resolution of ∼2 Hz. Last, while the sampling rate during SIMI94 was 1000 Hz, the data was bandpass filtered between 1 and 350 Hz during acquisition, so only these frequencies are presented in the results. Similarly, although the sampling rate during ICEX16 was 12 000 Hz, only results below 350 Hz are shown in this section to directly compare with SIMI94 results. The k–f beamforming outputs are plotted for both datasets to estimate the self noise level of both arrays. The frequency limits for these plots [Figs. 6(a) and 6(b)] correspond to the spatial aliasing frequency limit constrained by the respective array

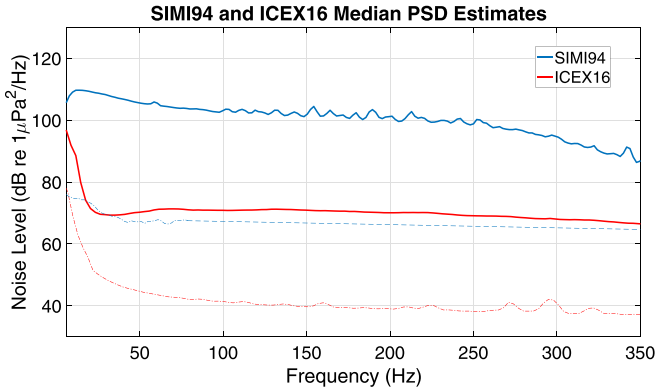

FIG. 5. (Color online) SIMI94 and ICEX16 median PSD estimates. Dotted-dashed lines show estimated array self noise derived from k–f beamforming; values above 80 Hz for SIMI94 are extrapolated.

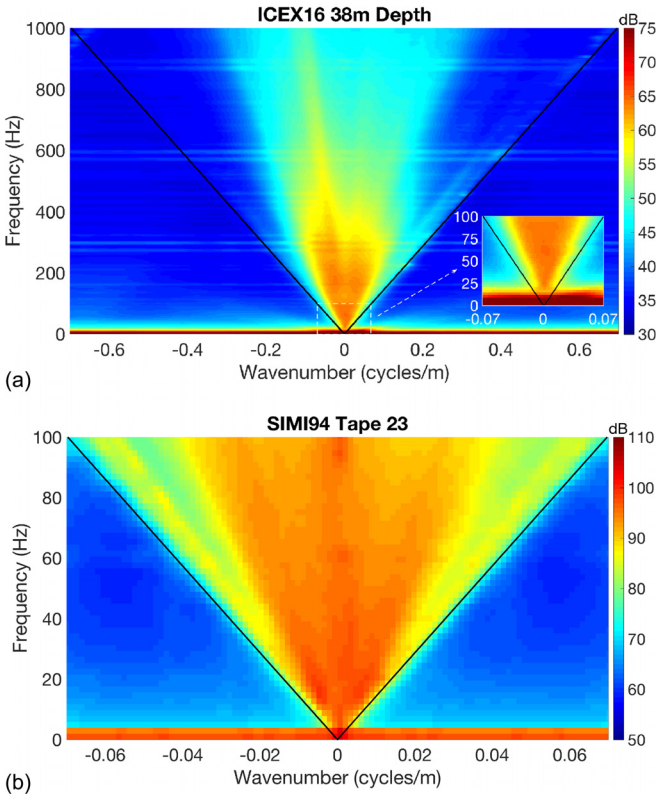

FIG. 6. (Color online) (a) ICEX16 k–f beamforming output showing unaliased frequencies below 1000 Hz; zoomed-in plot shows 0–100 Hz to directly compare with SIMI94. (b) SIMI94 k–f beamforming output showing unaliased frequencies below 100 Hz. For both cases, the sound speed assumed for the boundary of the propagating cone is 1435 m/s. Note the dB scale difference in the two plots.

spacings (100 Hz for SIMI94 and 1000 Hz for ICEX16). The array self noise estimates (shown in dot-dashed lines in Fig. 5) are determined by calculating the mean noise level outside the acoustic cone at different frequencies. For SIMI94, the array self noise levels above 80 Hz are extrapolated from the level at 80 Hz as starting at that frequency, aliasing effects begin to contaminate the non-propagating region of the k–f plot.

B. Results and discussion

As shown in Fig. 4(a), during ICEX16, ambient noise level below 25 Hz is much higher than levels at higher frequencies. The median PSD estimate reaches close to 100 dB then stabilizes to around 70 dB after 25 Hz (Fig. 5). No known frequency filtering was applied to the data during acquisition, thus, the excess in power at low frequencies is likely caused by array self-noise such as cable strum. This hypothesis is supported by k–f beamforming [Fig. 6(a)]—below 25 Hz, the noise level within and outside of the acoustic cone is much higher compared to other frequencies. In contrast to the ICEX16 data, SIMI94 tape 23 spectrogram [Fig. 4(b)] shows many persistent, high level bands at distinct frequencies that create spikes in the PSD estimate (Fig. 5). The peak at 60 Hz is caused by interference from the camp generators; the cause for the higher frequency peaks is unclear but is likely noise from other man-made sources because of their narrow bandwidth. However, this theory can not be confirmed by k–f beamforming because the

frequencies in question exceed the spatial aliasing frequency limit. Figure 5 also shows that the ambient noise level during SIMI94 is about 30 dB higher than ICEX16—the level decreases slightly with an increase in frequency but generally remains between 100 and 110 dB. These values are high compared to previously published ambient noise measurements from the Arctic region at this frequency band (typically 50–80 dB)[20] but are similar to the results shown in a prior study of the same SIMI94 data by Stamoulis.[21] Array self noise estimates derived from k–f beamforming shows that the noise floor of the SIMI94 array is quite high and is also roughly 30 dB higher than that for ICEX16. The cause of this high noise floor is possibly due to array self noise or some kind of spatially uncorrelated environmental noise as no additional processing (such as a gain) was applied to the data except for the bandpass filter mentioned previously. Thus, with this high noise floor, it is difficult to conclude that the ambient noise level during SIMI94 was actually higher than ICEX16. However, later analysis does suggest that the ice cover was more acoustically active during SIMI94 than ICEX16.

IV. VERTICAL DIRECTIONALITY ANALYSIS AND MODELING

A. Conventional beamforming

To compare the ambient noise spatial distribution during SIMI94 and ICEX16, conventional beamforming is used to analyze the noise vertical directionality. For SIMI94, the data is beamformed between 80 and 100 Hz so that the output has adequate spatial resolution without encountering aliasing. For the same reason, the ICEX16 data is beamformed between 800 and 900 Hz. ICEX16 data collected at 138 and 238 m depth are also analyzed and compared with SIMI94 because of their deeper depths, although there are only about 20 min of data for these depths. For both the SIMI94 and ICEX16 datasets, the beamforming outputs have frequency resolution of ∼0.2 Hz, temporal resolution of ∼2 s, and spatial mainlobe 3-dB-down-beamwidth of ∼2 degrees.

Figure 7(a) shows the average vertical noise directionality over 6 h of data from SIMI94 tape 23. Noise level peaks near the horizontal plane at 0 degrees elevation (up: +90 degrees; down: −90 degrees). In addition, Fig. 7(b) shows that the noise contains numerous tonal bands that vary in frequency with time and are prominent near the horizontal plane. Because of the meandering pattern of these tonal bands in frequency, they are not likely caused by artificial camp noise like the peaks observed in the PSD estimates (Fig. 5). Rather, their source is likely the ice cover. Xie and Farmer[22] have noted that intermittent pure tones are generated by shearing and rubbing of adjacent ice masses and that ice of different thicknesses resonates at different frequencies. Since the tones observed here are persistent with time, one possible explanation for them is that the compact ice cover during SIMI94 experienced constant shear stress as ice masses of variable thicknesses persistently rubbed against each other; furthermore, the ice was thick (≥2 m) and strong enough during SIMI94 to maintain this pressure to generate these tonal bands instead of ridging or breaking apart.

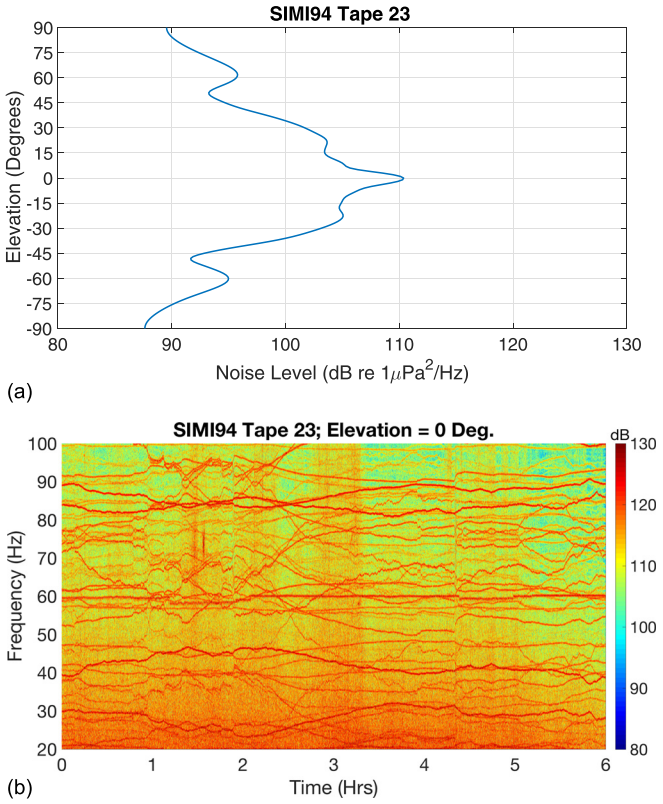

FIG. 7. (Color online) SIMI94 noise vertical directionality. (a) Profile generated by averaging the beampower in time and between 80 and 100 Hz. (b) Beampower at horizontal for different frequencies and times. Meandering tones that vary with frequency and persist with time are observed. Note that the frequency axis is extended down to 20 Hz to show that these tones occur at lower frequencies as well. The non-frequency varying, persistent tone at 60 Hz is due to camp generator noise.

In contrast to the SIMI94 results, vertical noise directionality during ICEX16 does not peak at 0 degrees elevation. Instead, with the array center at 38 m depth, the profile peaks at around −10 degrees; with the array center at 138 and 238 m depths, the vertical directionality profiles show two peaks near ±15 degrees and a noise notch at the horizontal [Fig. 8(a)]. Furthermore, Figs. 8(b), 8(c), and 8(d) show that persistent tonal bands are not observed during ICEX16 at the peak elevations between 800 and 900 Hz (nor do they exist at other elevations and frequencies). This difference suggests that unlike the ice during SIMI94, the thinner ice masses during ICEX16 (∼1 m) could not sustain constant shear and was more likely to fracture or build ridges instead of rubbing past each other to produce tones. Thus, the difference in the existence of tones between SIMI94 and ICEX16 could be the result of a change in ice cover property.

B. Surface source distribution modeling

To better understand why ambient noise during SIMI94 and ICEX16 exhibit their respective vertical directionality profiles, Figs. 7(a) and 8(a) are compared with modeled vertical noise directionality profiles generated using the acoustic wavenumber integration software, OASES.[23] The underlying model used for generating surface noise is the Kuperman–Ingenito (KI) model,[24] which assumes an infinite distribution of

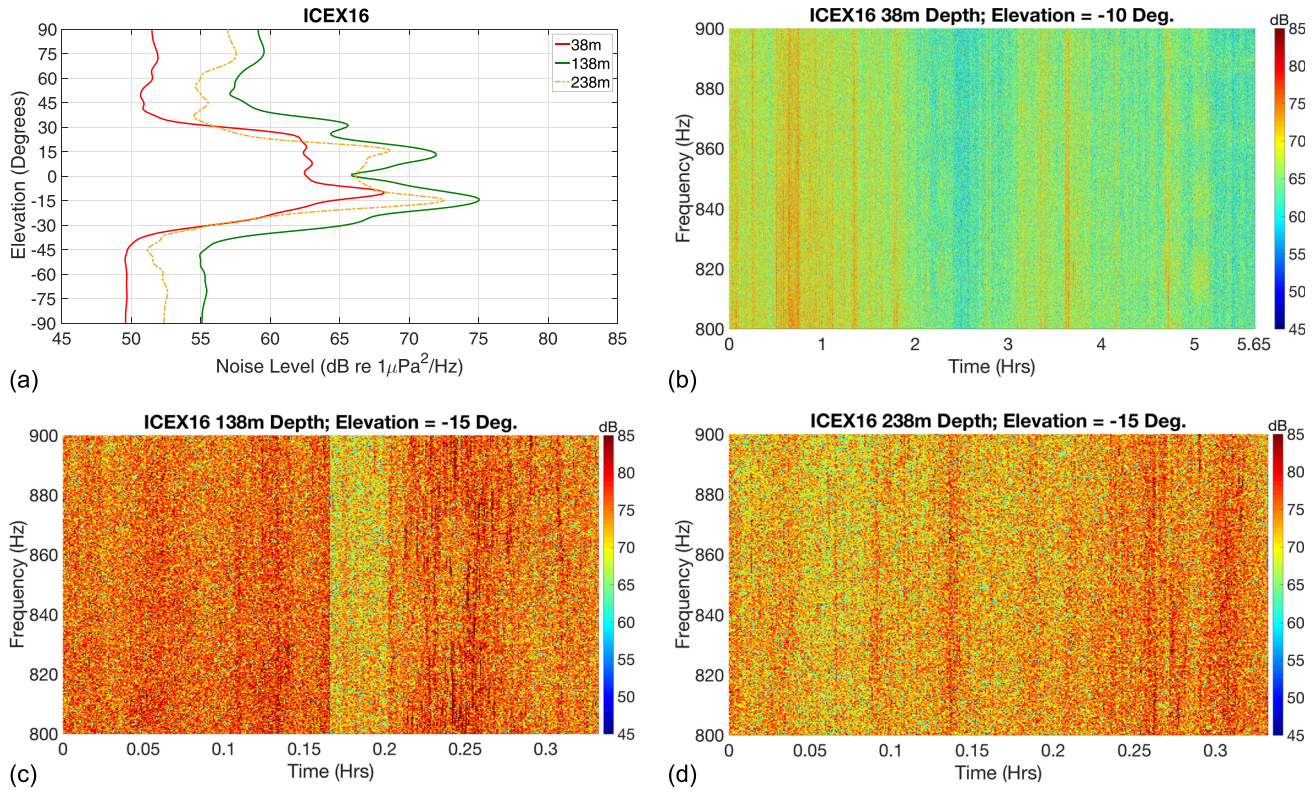

FIG. 8. (Color online) ICEX16 noise vertical directionality. (a) Vertical noise directionality profiles at 38, 138, and 238 m depths. All profiles are generated by averaging the beamformer output in time and between 800 and 900 Hz. (b)–(d) Beampower at −10 or −15 degrees elevation vs frequency and time with array at 38, 138, and 238 m depths. No meandering tones are observed in this case between 800 and 900 Hz. Although not shown, results from other frequencies and elevations angles also do not show meandering tones. Note that at 138 and 238 m depths, the time axis is shortened because there were only about 20 min of data collected. Data at 138 m consist of two disjoint segments of equal length, which is why there is a discontinuity in (c).

monopole sources just below a pressure release surface. For our model, a surface ice layer ($C_{compressional} = 3600$ m/s, $C_{shear} = 1800$ m/s, $\rho = 0.9$ kg/m^3;[25] 2 m thickness for SIMI94, 1 m thickness for ICEX16) with root-mean-square (rms) interface roughness of 0.2 m and roughness correlation length of 20 m is included with the KI source distribution placed $\lambda_{top}/30$ below the ice. The SSP during SIMI94 and ICEX16 (Fig. 1) are used as environmental input, respectively, with a solid bottom half-space below 3000 m ($C_{compressional} = 2200$ m/s, $C_{shear} = 1500$ m/s, $\rho = 2.9$ kg/m^3). The model source frequency is set between 80 and 100 Hz for SIMI94 and between 800 and 900 Hz for ICEX16 to match their respective beamforming frequencies. Only waterborne noise is accounted for by the model to eliminate noise with bottom bounces (but not those that skim the bottom) as they are heavily attenuated by bottom interactions in nature.

Figure 9 shows that for SIMI94, both the modeled and measure vertical directionality profiles peak near the horizontal. This suggests that the KI model could be a valid description of the SIMI94 ambient noise environment. In comparison, the same figure shows that the modeled profiles differ significantly from the measured ICEX16 profiles at all depths. Peak elevation angles in the modeled profiles are positioned closer to the horizontal plane and, although they do show a notch at 0 degrees elevation, the extent of this notch is more confined compared to the measured profiles. This difference suggests that the assumed source distribution (plane of monopoles near the surface) is not a valid description of the source distribution during ICEX16. Furthermore, comparing the modeled profiles of SIMI94 and ICEX16 with each other illuminates the extent that the Beaufort Lens affects ambient noise propagation. Since the increase in SSP due to the Beaufort Lens is included in generating the modeled profiles for ICEX16 but not SIMI94, the resultant difference between the modeled profiles of the two experiments shows that the Beaufort Lens is responsible for creating the noise notch at horizontal during ICEX16. Pairing this result with the observed mismatch between measured and modeled profiles for ICEX16 further suggests that the Beaufort Lens is not the sole contributor to the measured change in vertical noise directionality between SIMI94 and ICEX16; again, the surface source distribution during ICEX16 must have changed from SIMI94.

As mentioned above, the ice cover in the current Arctic is younger and more prone to ridging as compared to the past.[3] Consequently, surface noise generation during ICEX16 may have been dominated by ridging processes which occur at discrete locations rather than uniformly distributed over the entire ice sheet. To test this hypothesis, OASES is again used to generate vertical noise directionality profiles with the underlying model of a single monopole source near the surface moving in a straight line to simulate a ridge formation. The same environmental parameters are used as in the KI source distribution case for ICEX16; the discrete source is again placed $\lambda_{top}/30$ below the ice sheet and moved from 3 to 50 km away from the VLA at 0.5 km intervals.

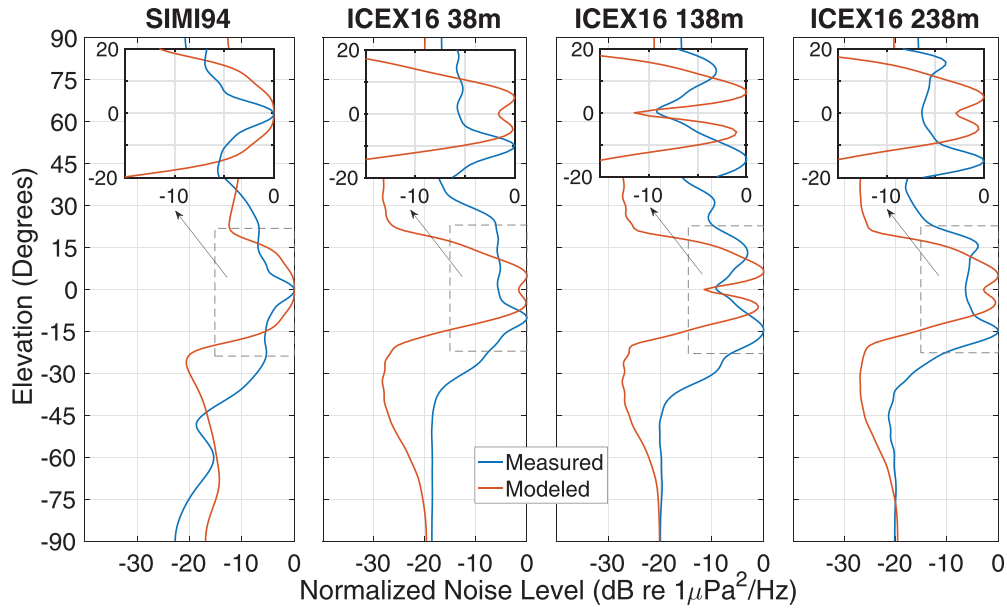

FIG. 9. Modeled (KI) vertical directionality profiles compared with measured SIMI94 and ICEX16 profiles. Peak elevation angle of the modeled profile matches with the measured profile for SIMI94 but not for ICEX16.

The set-up and output for the discrete source model is shown in Fig. 10. As the source moves along the line, the resultant vertical directionality profiles from all source locations are shown in the form of a contour plot. For all depths, as the source moves further away for the VLA, the peak elevation angle of the modeled output moves further away from horizontal and the noise notch at horizontal becomes more apparent. Thus, the output of this discrete source model appears to be more similar to the measured profiles for ICEX16 than the previous KI source distribution. Particularly, as shown on the left side of Fig. 10, for 38 m depth, the averaged output between 26 and 27 km matches the measured output most closely, suggesting that ambient noise recorded during this time is dominated by ridging activity at that distance. For 138 and 238 m, the averaged model output between 36 and 37 km and 46 and 47 km closely match the measured outputs, respectively, suggesting that ambient noise measured during these times are dominated by ridging activity at these respective distances. However, its important to note that this new model is possibly just one component of a more complicated explanation for the vertical directionality profiles observed in ICEX16;

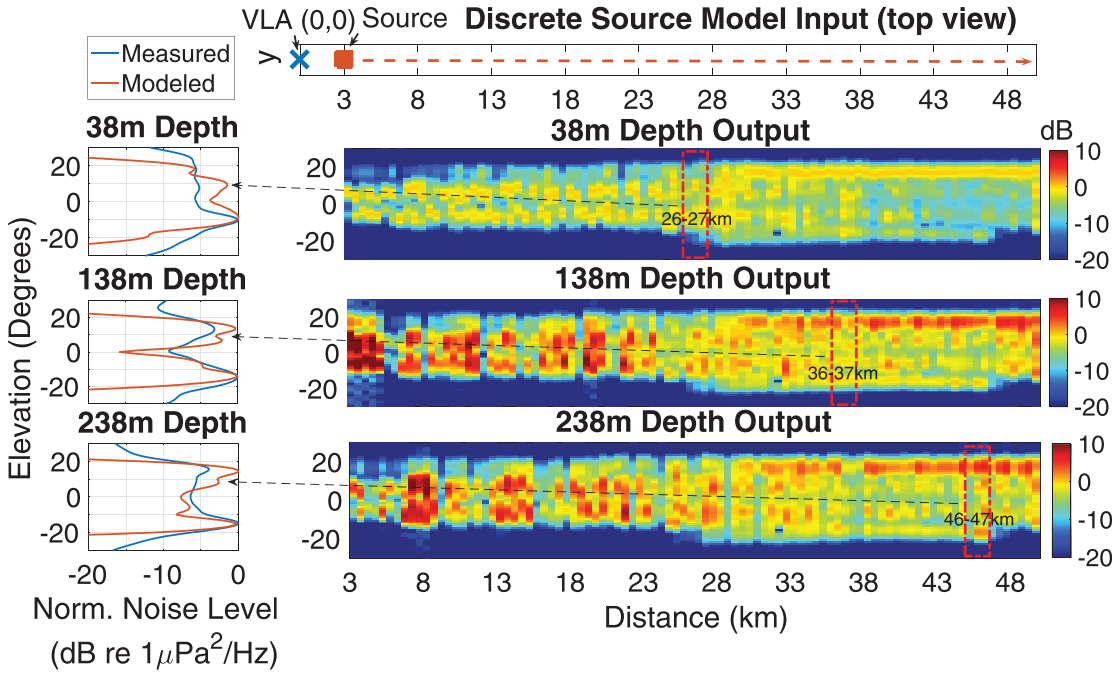

FIG. 10. Discrete source model setup and output for ICEX16. Top plot shows the model set-up. On the right, model output is shown with respect to source distance. On the left, averaged model output between the indicated distances on the contour plot are compared with measured profiles for ICEX16 at the respective depths.

the entire ensemble of noise generation during ICEX16 may be more complex. Nonetheless, the positive results suggest that the proposed model is a plausible explanation.

V. TEMPORAL STATISTICS OF TRANSIENT ICE EVENTS

A. Method

Analysis of the temporal distribution of transient ice events and their inter-arrival times allows for a better understanding of ice activity as a function of time and the mechanisms by which transient events are generated. Unsurprisingly, the temporal statistics of ambient noise observed during SIMI94 and ICEX16 differ significantly. Data from both ICEX16 (38 m depth) and SIMI94 (tape 23) are examined in this analysis. An event detection algorithm developed based on a method by Zakarauska and Thorleifson[26] and Zakarauska[27] is used to find transient events in both datasets. The algorithm requires three parameters (w, r, p_{thres}) and looks for improbable clusters of high amplitude peaks within the data time series. Briefly, it works as follows:

(1) Form a histogram of the peak amplitudes of the input time series.
(2) Set the amplitude value exceeded by r% of the histogram as a threshold, m.
(3) Partition the time series into adjoining segments of w peaks; within each segment, count the number of peaks, N, whose amplitude exceed m.
(4) Calculate the probability of having at least N peaks from the top r% of the histogram within a window of w peaks as a sum of binomial distributions, i.e., $P = \sum_{i=N}^{w} \binom{w}{i} r^i (1-r)^{(w-i)}$.
(5) If P is less than the chosen threshold probability p_{thres}, then the window contains an event and the peaks within the window that have amplitude greater than m are identified.
(6) Consecutive peaks that are less than 0.05 s apart are grouped into a single compound event. This threshold is set based on the description of transient event types in previous studies by Chen[28] and Stamoulis,[21] where different arrivals within the same event are typically less than 0.05 s apart.

The algorithm parameters used to analyze both datasets are $w = 10$, $r = 1\%$, and $p_{thres} = 0.00001$. $w = 10$ is chosen because an impulsive transient event contains, typically, less than 10–20 peaks.[21,28] If w is too large, shorter events may be missed because the likelihood of having a few large peaks within a long window may still be fairly high. Thus, to be conservative, a small value of 10 is chosen. However, it is also unlikely for a transient event to have only 1 or 2 peaks and ideally, p_{thres} should be small so that the number of false alarms is kept to a minimum; $p_{thres} = 0.00001$ seems to be a reasonable threshold. r is chosen in complement to the other two parameters so that, as shown in Table I, as N increases to more than two peaks within a window of ten, the window would be selected to contain a transient. As another check for false alarms, this method is applied to data on all 32 channels for both datasets and detected transients are only confirmed to be events if they appear on at least 3/4 of the channels. After event selection, the beginning and end times of each event are documented.

TABLE I. Probability of N or more peaks with amplitude greater than the top r% of the PDF in a sample of ten peaks.

	$r = 10\%$	$r = 5\%$	$r = 1\%$	$r = 0.5\%$	$r = 0.1\%$
$N = 1$	0.264	0.086	0.004	0.001	4.476×10^{-5}
$N = 2$	0.070	0.012	1.138×10^{-4}	1.461×10^{-5}	1.194×10^{-7}
$N = 3$	0.013	0.001	2.001×10^{-6}	1.281×10^{-7}	2.089×10^{-10}

Because the ambient noise level increases towards lower frequencies, the data must be bandpass filtered into separate frequency bands before being processed by the event selector or higher frequency events may be missed.[26,27] Thus, for both datasets, the time series are filtered into three octave bands between 40 and 320 Hz. The narrow-band inference in the hundred Hertz band observed in the SIMI94 data (Fig. 5) should not affect the output of the event selector because they are persistent with time and the event selector is focused on large amplitude transient events.

B. Results and discussion

The number of transient events detected from the ICEX16 and SIMI94 datasets are tallied in Table II. As shown, the number of events increases with frequency for both datasets. This result suggests that as frequency increases, transient events contribute more and more to the total ambient noise environment, which agrees with the findings of a previous study by Zakarauska and Thorleifson.[26]

After the events are detected and their start and end times recorded, the inter-arrival time between events from ICEX16 and SIMI94 are compared to gain a better understanding of the temporal density and distribution of the detected transients. These times are calculated by subtracting the end time of one event from the start time of the next. Only one previous study has been found to characterize inter-arrival times between transient events.[16] In that study, a J-shaped gamma distribution is found to best describe the statistical spread of inter-arrival times if very large outliers (>280 s) are excluded. However, it may be natural to have very large inter-arrival times if the weather conditions are calm and the ice cover experiences low environmental forcing. A more natural way to characterize inter-arrival times may be to view the occurrence of transient events as a clustering process. Within a cluster, the inter-arrival times are short but large gaps may separate consecutive clusters. To visualize and verify this clustering process, the data time series are segmented into 1 min bins and the number of events detected within each bin is counted. The results for both datasets are presented in Fig. 11. This plot highlights

TABLE II. Number of detected transient events in each frequency band.

	$f = 40$–80 Hz	$f = 80$–160 Hz	$f = 160$–320 Hz
ICEX16	43	86	260
SIMI94	173	451	1043

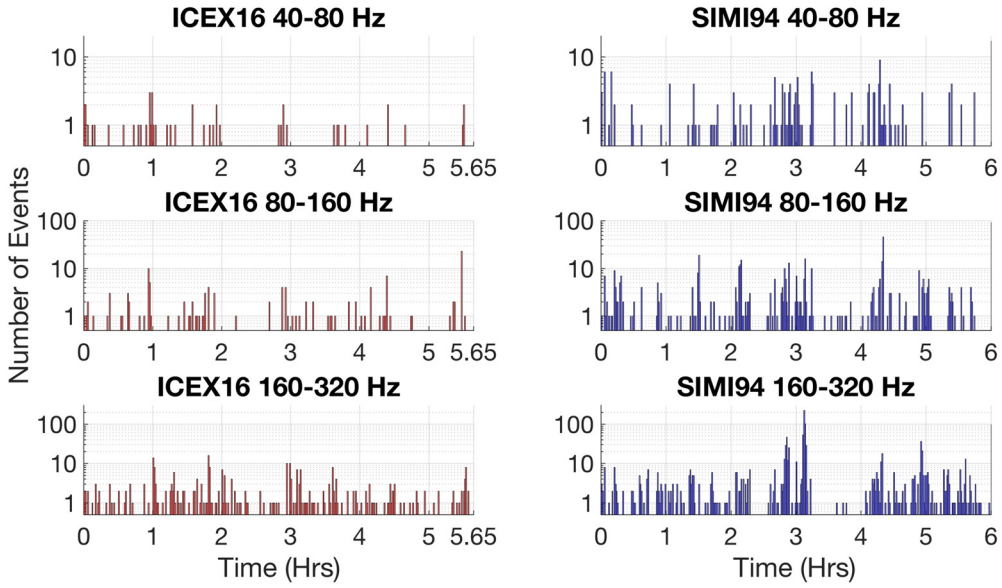

FIG. 11. (Color online) Temporal distribution of transient events during ICEX16 (left) and SIMI94 (right) at three frequency bands. Plots show the clustering of events and time gaps that separate the clusters.

that the transient events do indeed occur in clusters that are separated by gaps, with a cluster defined as any period of time during which at least one event occurs in each 1 min bin and a gap defined as any period of time during which no events occur in each 1 min bin.

To better describe the difference between transient event activity during SIMI94 and ICEX16, the statistical distribution of the cluster and time gap lengths, as well as the number of events within each cluster for both datasets are plotted and shown in Fig. 12. The gap length distribution of the two datasets are similar at all three frequency bands, meaning that event clusters occurred at similar rates during both experiments. However, event clusters are likely to be longer during SIMI94 than ICEX16 as shown by the distribution of event cluster lengths. The number of transient events within each cluster are also likely to be greater during SIMI94. These results suggest that if an event cluster can be assumed as a period of high ice activity, then SIMI94 and ICEX16 have comparable statistics regarding the occurrence of such high activity periods. However, within such a period, the ice cover during SIMI94 is likely to be more acoustically active and produce more transient events than the ice cover during ICEX16. The reason for this difference may simply be that environmental forces such as wind or temperature were

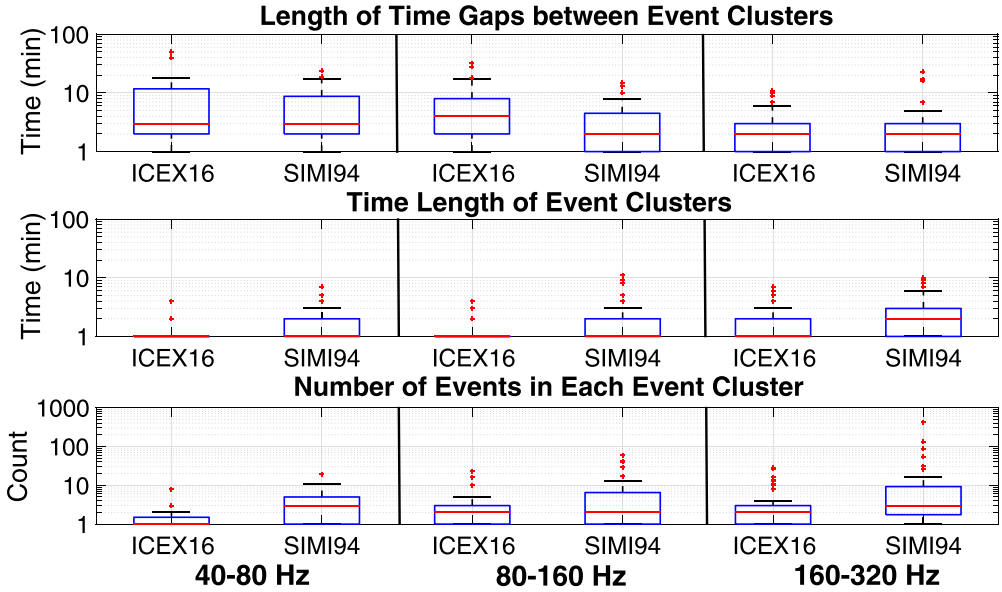

FIG. 12. (Color online) Statistical distribution of time gap lengths, cluster lengths, and number of events in each cluster during ICEX16 and SIMI94 at three frequency bands. Red lines represent the median, box edges represent the 25th and 75th percentiles, whiskers extend to the 1st and 99th percentiles, and red crosses signify extreme values that are much larger than the rest of the distribution. Gap lengths of the two datasets have comparable distributions (top). Although the median values are similar, event clusters are more likely to be longer during SIMI94 than ICEX16 (middle). The number of transient events within each cluster are also likely to be greater during SIMI94 at all three frequency bands (bottom).

more prominent during SIMI94. However, another plausible explanation may result from the proposed change in the surface noise source distribution between the two experiments from Sec. IV. More transient events would be expected to be generated from a continuous and uniform distribution of sources, as is suspected to be the case during SIMI94, than from a few distinct sources located at specific locations, as is suspected to be the case during ICEX16. Thus, the temporal statistics of transient noise appear to reinforce the proposed noise generation models in Sec. IV.

VI. CONCLUSIONS

Ambient noise recorded during ICEX16 and SIMI94 is compared to study how environmental changes in the Arctic ocean have altered the underwater ambient noise environment. Both datasets were collected with 32 element VLAs under packed ice conditions in the Beaufort Sea. Spectral analysis shows that ambient noise during SIMI94 in the 20–350 Hz band is ~30 dB louder than ICEX16. However, this difference may be due to higher array self noise during the SIMI94 experiment.

Conventional beamforming shows that the vertical directionality of ambient noise during SIMI94 is focused near the horizontal plane. In comparison, ambient noise during ICEX16 is more spread in elevation with peaks near −10 degrees at 38 m depth and near ±15 degrees at 138 and 238 m depths. Modeling with OASES demonstrates that unlike the SIMI94 data, ambient noise from ICEX16 is not well described by the vertical noise directionality profile generated with the Kuperman-Ingenito model, which assumes a uniform distribution of monopole sources near the surface. Instead, a moving monopole source at discrete distances models the ICEX16 data more closely. This result suggests that the ambient noise during ICEX16 is dominated by ice noise sources at discrete ranges—such as localized ridge building events, in contrast to the historical Arctic model of a more continuous distribution of sources.

Temporal analysis of transient events detected within both datasets demonstrates that ice events during both experiments may be modeled as a clustering process. The median time gap lengths between event clusters are comparable between the two datasets; however, cluster lengths and number of events in each cluster are greater during SIMI94 than ICEX16, suggesting that when the ice cover is active, more transient events are likely to be produced during SIMI94 than ICEX16. This result appears to reinforce the new surface noise model proposed for ICEX16.

Future work will focus on further validating the changes in the Arctic ambient noise environment and the surface noise source distribution proposed in this paper for ICEX16. Specifically, time delays between the arrival of each detected event at different hydrophones in the VLA allow for the directionality of each event to be calculated. Assuming direct paths between the source of each event and the VLA, the position of each event can be mapped and their spatial distribution can be compared to the proposed noise generation model. In addition, examination of the Beaufort Sea region environmental data such as temperature, wind speed, and ice cover thickness during the time of SIMI94 and ICEX16 will help to verify the findings of this study.

ACKNOWLEDGMENTS

The authors would like to express their deep gratitude to the large number of individuals that made the research presented in this paper possible. First and foremost, Dr. B. Headrick, ONR Code 322OA for his effort in raising funding for the MIT participation in ICEX16 from the ONR Experimentation Program lead by Dr. T. Killian, and for funding the preparation and noise processing through the ONR MURI Information Content of Ambient Noise. Additional funding for the subsequent analysis was provided by DARPA STO under the FAST Program, lead by Dr. J. Kamp and by the National Science Foundation Graduate Research Fellowship under Grant No. 2389237. Of course, the funding for the SIMI94 MIT involvement provided by Dr. T. Curtin, ONR Code 322OM is appreciated as well. In addition to the funding, the MIT participation in ICEX16 would not have happened without the support of CAPT Carl Hartsfield and ADM M. Connor of COMSUBFOR who issued the invitation to MIT in the first place, and subsequently provided strong support for raising the funding. The effort of the entire MIT ICEX16 team, LT. S. Carper, Mr. T. Howe, Dr. T. Schneider, Gobysoft LLC, without which the data collection would not have been successful, is highly appreciated as well. The effort of Dr. E. Fischell in upgrading and preparing the acquisition system was crucial, as well as her assistance in editing the manuscript. Professor A. Baggeroer was instrumental in raising Navy support for the ICEX16 participation, and provided invaluable advice on the signal processing. Last, the thoughtful comments and suggestions from the reviewers were greatly appreciated as well. This work was supported by ONR, NSF, and DARPA STO.

[1]R. Kwok and D. A. Rothrock, "Decline in Arctic sea ice thickness from submarine and ICESAT records: 1958-2008," Geophys. Res. Lett. **36**, L15501, https://doi.org/10.1029/2009GL039035 (2009).
[2]K. E. Frey, G. W. K. Moore, L. W. Cooper, and J. M. Grebmeier, "Divergent patterns of recent sea ice cover across the Bering, Chukchi, and Beaufort seas of the Pacific Arctic region," Prog. Oceanogr. **136**, 32–49 (2015).
[3]J. Maslanik, J. Stroeve, C. Fowler, and W. Emery, "Distribution and trends in Arctic Sea ice age through spring 2011," Geophys. Res. Lett. **38**, L13502, https://doi.org/10.1029/2011GL047735 (2011).
[4]J. M. Toole, M. L. Timmermans, D. K. Perovich, R. A. Krishfield, A. Proshutinsky, and J. A. Richter-Menge, "Influences of the ocean surface mixed layer and thermohaline stratification on Arctic sea ice in the central Canada basin," J. Geophys. Res. **115**, C10018, https://doi.org/10.1029/2009JC005660 (2010).
[5]Woods Hole Oceanographic Institution, "Ice-tethered profiler program," http://www.whoi.edu/itp (Last viewed 1/22/2019).
[6]T. Howe, "Modal analysis of acoustic propagation in the changing Arctic environment," Master's thesis, MIT, Cambridge, MA, 2015.
[7]H. Schmidt and T. Schneider, "Acoustic communication and navigation in the new Arctic: A model case for environmental adaptation," in *Proceedings of the 2016 IEEE Third Underwater Communications and Networking Conference (UComms)*, Lerici, Italy (August 30–September 1, 2016), pp. 1–4.
[8]A. R. Milne and J. H. Ganton, "Ambient noise under Arctic sea ice," J. Acoust. Soc. Am. **36**, 855–863 (1964).
[9]N. C. Makris and I. Dyer, "Environmental correlates of pack ice noise," J. Acoust. Soc. Am. **79**(5), 1434–1440 (1986).

[10]N. C. Makris and I. Dyer, "Environmental correlates of Arctic ice edge noise," J. Acoust. Soc. Am. **90**, 3288–3298 (1991).
[11]E. H. Roth, J. A. Hildebrand, and S. M. Wiggins, "Underwater ambient noise on the Chukchi Sea continental slope from 2006–2009," J. Acoust. Soc. Am. **131**(1), 104–110 (2012).
[12]G. B. Kinda, Y. Simard, C. Gervaise, J. I. Mars, and L. Fortier, "Under-ice ambient noise in eastern Beaufort sea, Canadian Arctic, and its relation to environmental forcing," J. Acoust. Soc. Am. **134**(1), 77–87 (2013).
[13]G. B. Kinda, Y. Simard, C. Gervaise, J. I. Mars, and L. Fortier, "Arctic underwater noise transients from sea ice deformation: Characteristics, annual time series, and forcing in Beaufort sea," J. Acoust. Soc. Am. **138**(4), 2034–2045 (2015).
[14]R. F. Dwyer, "A technique for improving detection and estimation of signals contaminated by under ice noise," J. Acoust. Soc. Am. **74**(1), 124–130 (1983).
[15]J. Veitch and A. Wilks, "A characterization of Arctic undersea noise," J. Acoust. Soc. Am. **77**, 989 (1985).
[16]M. Townsend-Manning, "Analysis of central Arctic noise events," Master's thesis, MIT, Cambridge, MA, 1987.
[17]P. J. Stein, "Interpretation of a few ice event transients," J. Acoust. Soc. Am. **83**(2), 617–622 (1988).
[18]P. Zakarauskas and J. M. Thorleifson, "Directionality of ice cracking events," J. Acoust. Soc. Am. **89**(2), 722–734 (1991).
[19]M. V. Greening and P. Zakarauskas, "Spatial and source level distributions of ice cracking in the Arctic Ocean," J. Acoust. Soc. Am. **95**(2), 783–790 (1994).
[20]E. Ozanich, P. Gerstoft, P. F. Worcester, M. A. Dzieciuch, and A. Thode, "Eastern Arctic ambient noise on a drifting vertical array," J. Acoust. Soc. Am. **142**(4), 1997–2006 (2017).
[21]C. Stamoulis, "Analysis of ice-induced acoustic events in the central Arctic," Ph.D. dissertation, MIT, Cambridge, MA, 1997.
[22]Y. Xie and D. M. Farmer, "The sound of ice break-up and floe interaction," J. Acoust. Soc. Am. **91**(3), 1423–1428 (1992).
[23]H. Schmidt, "Oases: Ocean acoustic and seismic exploration synthesis," MIT, http://lamss.mit.edu/lamss/pmwiki/pmwiki.php?n=Site.Oases (Last viewed 1/22/2019).
[24]W. A. Kuperman and F. Ingenito, "Spatial correlation of surface generated noise in a stratified ocean," J. Acoust. Soc. Am. **67**(6), 1988–1996 (1980).
[25]G. Hope, H. Sagen, E. Storeim, H. Hobæk, and L. Freitag, "Measured and modeled acoustic propagation underneath the rough Arctic sea-ice," J. Acoust. Soc. Am. **142**, 1619 (2017).
[26]P. Zakarauskas and J. M. Thorleifson, "Automatic extraction of spring-time Arctic ambient noise transients," J. Acoust. Soc. Am. **90**(1), 470–474 (1991).
[27]P. Zakarauskas, "Detection and localization of nondeterministic transients in time series and application to ice-cracking sound," Digital Signal Process. **3**, 36–45 (1993).
[28]C. F. Chen, "Analysis of marginal ice zone noise events," Ph.D. dissertation, MIT, Cambridge, MA, 1990.